PCCP

Precipitation and surface adsorption of metal complexes during electropolishing. Theory and characterization with X-ray nanotomography and surface tension isotherms

Journal:	*Physical Chemistry Chemical Physics*
Manuscript ID:	CP-ART-06-2015-003431.R1
Article Type:	Paper
Date Submitted by the Author:	25-Jul-2015

Complete List of Authors:	Kornev, Konstantin; Clemson University, School of Materials Science and Engineering Nave, Maryana; Clemson University, Materials Science & Engineering Chen-Wiegart, Yu-chen Karen; Brookhaven National Lab, Wang, Jun; Brookhaven National Lab,

Precipitation and surface adsorption of metal complexes during electropolishing. Theory and characterization with X-ray nanotomography and surface tension isotherms

Maryana I. Nave[a], Yu-chen Karen Chen-Wiegart[b], Jun Wang[b] and Konstantin G. Kornev[a]*

[a]Department of Materials Science and Engineering, Clemson University, Clemson, SC 29634, USA

[b]Photon Sciences Directorate, Brookhaven National Laboratory, Upton, New York 11973, USA

ABSTRACT. Electropolishing of metals often leads to super-saturation conditions resulting in precipitation of complex compounds. The solubility diagrams and Gibbs adsorption isotherms of the electropolishing products are thus very important to understand the thermodynamic mechanism of precipitation of reaction products. Electropolishing of tungsten wires in aqueous solutions of potassium hydroxide is used as an example illustrating different thermodynamic scenarios of electropolishing. Electropolishing products are able to form highly viscous films immiscible with surrounding electrolyte or porous shells adhered to the wire surface. Using X-ray nanotomography, we discovered a gel-like phase formed at the tungsten surface during

electropolishing. The results of these studies suggest that the electropolishing products can form a rich library of compounds and the surface tension of electrolyte is affected by the metal oxide ions with alkali-metal complexes.

INTRODUCTION

Electropolishing is a popular inexpensive method for smoothing metal surfaces, micromachining, and sharpening metal wires [1-3]. In electropolishing, the metal is immersed in an electrolyte solution and, upon application of a voltage; the metal undergoes an electrochemical reaction resulting in the material removal. As a result, a rough metal surface can be significantly smoothed out and the wire tips can be sharpened to the nanometer radii [4-10]. Currently, the available electropolishing techniques take advantage of the convection-limited electropolishing (CLE) when the flowing electrolyte facilitates the removal of ions from the metal surface [4, 6, 11-14]. In many cases, the flowing film is oversaturated with the products of electrochemical reaction and may form a phase which is immiscible with the surrounding electrolyte. In attempt to reduce the influence of the flowing film on electropolishing, reserchers used magnetic field[15, 16], rotating electrodes[17, 18], and some other means[1, 2].

This work aims to understand how the solution properties change during electropolishing. Tungsten was chosen as an example of an important metal: tungsten wires are used to make sharp probes for scanning tunneling microscopy[19], atomic force microscopy[13], field ion microscopy, Raman spectroscopy[20], nanolithography[21], micro/nano welding[22], etc[13, 23]. At the same time, electropolishing of tungsten wires is a challenging task. Tungsten electropolishing in aqueous environment leads to the formation of a rich library of compounds. These compounds

affect the process efficiency which depends on thermodynamic stability of electrolytes and their surface properties.

Therefore, in this paper, the main attention is given to the ion concentrations corresponding to the conventional conditions of tungsten electropolising in aqueous solutions of potassium hydroxide[14]. We construct the solubility diagrams and discuss the conditions leading to precipitation of tungsten-based compounds. The changes of surface tension of these electrolytes are related to the conditions of phase separation.

In electropiolishing of tungsten wires in aqueous solutions of potassium hydroxide, the tungsten wire is connected to a power supply and serves as an anode. As suggested by Kelsey [24], the anodic and cathodic electrochemical reactions can be summarized as following: $6H_2O + 6e^- \rightarrow 3H_2(g) + 6OH^-$, $W(s) + 8OH^- \rightarrow WO_4^{2-} + 4H_2O + 6e^-$. Tungsten oxidizes with continuous release of tungstate ions WO_4^{2-} into water changing the electrolyte composition. As shown recently, the amount of potassium hydroxide in solution influences the rate of electropolishing and significantly influences the solution stability: one can observe precipitation of different tungsten oxides and hydrates in the form of flakes and nuclei [23]. Since the surface and capillary effects are impostant for obtaining smooth and sharp tips of the tungsten wires [14], one has to pay a speciall attention to the change of surface tension of the electrolyte during electropolishing.

Knowing the dependence of surface tension on concentration of the electrolyte constituents one can obtain adsorption isotherms[25-37]. It is known that the electrolyte-air interface can either repel or attract ions to its surface[29, 35, 38]. If the ions are repelled, the adsorption of ions to the interface is called negative; this effect is manifested through an increase of surface tension. If the ions are attracted to the surface of the electrolyte, then the adsorption is called positive; the

surface tension decreases [36]. As the salt concentration increases, the surface tension does not always increase or decrease monotonously; sometimes it can go through a minimum. This Jones - Ray effect was discovered by Jones and Ray and continues to be an unsolved controversy [39-48] [41]. Thus, adsorption of multiple ions on the electrolyte surface is poorly understood and, to the best of our knowledge, it has never been studied in the electropolishing applications.

EXPERIMENTAL

Solutions preparation. Solutions were prepared by electropolishing of tungsten plates by the CLE technique described in refs [14, 23]. The tungsten square plate (15x15 mm) with thickness of 1.5mm served as an anode. The stainless steel rod with 15mm diameter and 50mm length was used as a cathode. Both electrodes were placed into a glass beaker with diameter of 20 mm and height of 25 mm and connected to a potentiostat CHI 660D (CH Instruments, Inc.). Then, a 1 ml of the freshly prepared 2M KOH electrolyte solution was added to the beaker using a 1ml syringe. In order to prepare solutions with different concentrations of the reaction products, tungsten was electropolished at the 10V DC potential for different periods of time for different periods of time. The salt concentration of 2M KOH and applied potential of 10V are typically used in conventional method of formation of tungsten probes[14, 23]. Therefore, we followed the most common conditions to reproduce the products of electrochemical reactions. Each time, at the end of the electopolishing, solutions were carefully collected and transferred into the glass vial using a 1ml syringe. The dependence of current versus time was saved for each experiment for further calculations of the mass loss of tungsten. Each experiment was performed with a freshly prepared KOH solution, every time in a new beaker.

When electric current passes through the electrolytic cell, the number of moles liberated during the reaction can be estimated using Faraday's law as: $m = Q/zF$, where Q is the total charge at time t, z = 6 is the tungsten valence number, and $F = 96485$ C/mol is Faraday's constant. The total charge Q is found by integrating the current: $Q = \int I(t)dt$. The concentration is determined as follows: $C_i = N_i / V$, where C_i, is defined as the amount of moles of the solute, N_i, divided by the volume of the solution, V. The number of moles was estimated from the overall electrochemical reaction $W + 2OH^- + 2H_2O \rightarrow WO_4^{2-} + 3H_2$ that shows that the reaction proceeds with oxidation of one mole of tungsten to one mole of tungstate ions.

Measurements of volumetric mass density. The density measurements were performed using a microbalance and a micropipette. For each solution, a drop of V=30μL was placed on the pan of the microbalance to measure the weight in mg. For each solution, five drops were measured to obtain the standard deviation of the measurements. The densities were calculated using the following equation $\rho=m/V$. The measured density of the 2M KOH solution was equal to $\rho_{2MKOH} = 1.0990 \pm 0.0024 g/cm^3$ and was in a good agreement with the density found in the literature [49].

Surface tension measurements. The surface tension measurements were performed using Kruss DSA10 instrument with 1.25mm needle diameter for all solutions. Once a glass syringe was filled with the solution a pendant drop was produced and images were recorded using the Kruss DSA software for further analysis. All measurements were carried out at the room temperature (. Five measurements were taken for each solution to get a standard deviation. The surface tension of water measured with this technique was equal to $\sigma_w = 71.82 \pm 0.38 mN/m$. The

surface tension of the 2M KOH was equal to $\sigma_{2MKOH} = 75.17 \pm 0.1 mN/m$. This value of surface tensions agrees fairly well with the surface tensions reported in the literature[28-30, 35, 50].

pH analysis. The pH was measured using a pH meter from Denver Instruments UltraBASIC US-10 and double checked with the pH strips.

SEM-EDS. The precipitates in solutions were filtered out and washed 5 times with the DI water. After that, they were left to dry in the air at room temperature for 24h. The precipitates appeared to have white dull color. They were analyzed using the FESEM-Hitachi S4800 scanning electron microscope equipped with the Oxford INCA Energy 200 Energy Dispersive Spectroscopy (EDS). The precipitates were mounted on aluminum stubs with carbon-graphite tape for fixation.

XRD. The X-ray diffraction (XRD) patterns were acquired using a Rigaku Ultima IV powder diffractometer equipped with Cu *Kα* radiation (λ=1.5418 Å) in the angular range from 10˚ to 80˚ *2θ*. The XRD measurements were carried out at the room temperature. The data was analyzed using PDXL software version 1.4.0.0.

Thermal analysis. The Thermal Gravimetric Analysis (TGA) was performed on TA Instruments TGA Q5000 V3.13 Build 261 with a ramp 10°C/min from 25°C to 400°C in nitrogen gas. First the sample was equilibrated at room temperature under nitrogen purge for 10 min prior to heating. The Differential Scanning Calorimetry (DSC) was performed on TA Instruments DSC Q1000 V9.9 Build 303. First the sample was equilibrated at 25°C followed by the temperature increase with the 10°C/min ramp to 400°C in helium gas. To analyze the data, the TA Instruments Universal Analysis 2000 V3.9A and 4.7A software was employed.

TXM nanotomography. The nanotomography with the transmission X-ray microscope (TXM) was performed on the samples prepared with the CLE technique at beamline X8C of National

Synchrotron Light Source, Brookhaven National Laboratory [51]. The schematic of the setup is shown in Figure 1, where the X-ray beam with the 8960 eV energy is focused by a capillary condenser on the tungsten wire. A Fresnel zone plate was used as an objective lens to form an image onto the CCD detector (2048 x 2048 pixels) with the camera binning 2 x 2 pixels or 4 x 4 pixels with a single pixel size of 20 nm. The images were continuously collected with the 1 s exposure time. This run resulted in the collection of 1441 projections with the 40 x 40 μm^2 field of view. After the measurements, the background was subtracted and an automatic alignment using the run-out correction system was applied. A standard filtered back-projection reconstruction algorithm was used to construct the 3D images [52]. Volume rendering was applied to the reconstructed image stacks using Avizo® program, VSG, version 8.0.

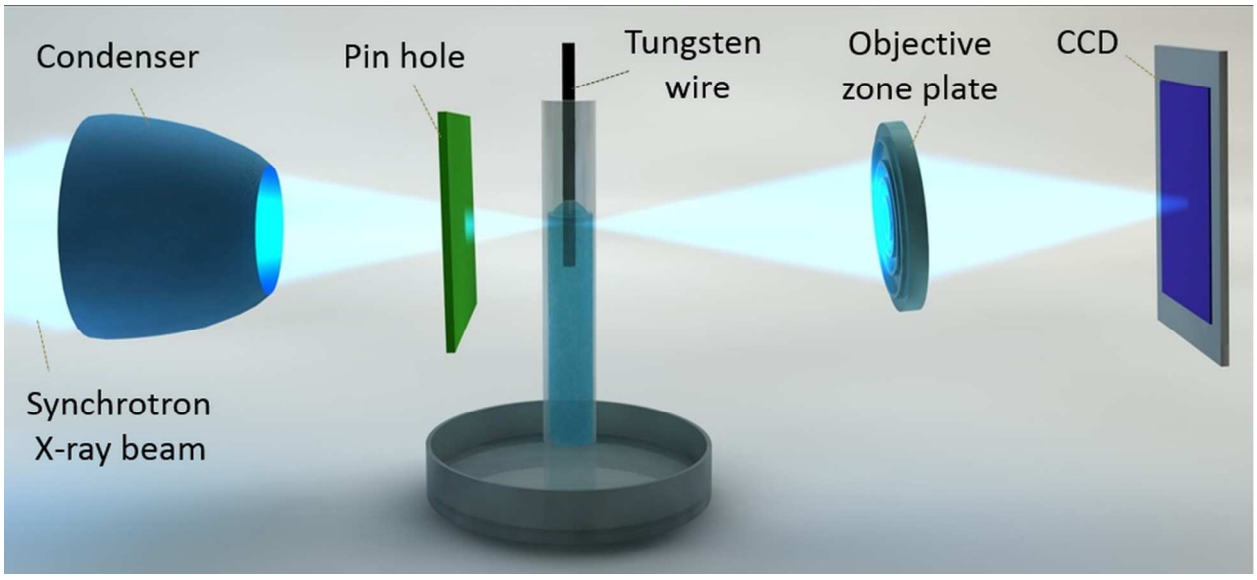

Figure 1. Schematic of the sample positioning on the transmission X-ray microscope (TXM). A tungsten wire was immersed in a Kapton tube filled with the electrolyte. The wire was connected to a battery and was placed on the sample stage. Rotating the stage, one acquires the necessary images further used for reconstruction of a 3D volume.

THEORY

Stability of the tungsten compounds in aqueous solutions

The stability of different tungsten compounds in aqueous solutions of potassium hydroxide can be determined using thermodynamics of chemical reactions [37, 53-55] . First, all possible chemical reactions are written down in the following form:

$$n_0 A_0 + n_1 A_1 + ... + n_r A_r = m_1 B_1 + ... + m_s B_s, \quad (1)$$

assuming that N_0 moles of A_0 solvent molecules are mixed with, N_1,…, N_i moles of A_1, … A_r solutes molecules that react on the left side, producing N'_1,…, N'_j moles of B_1, … B_s solutes molecules that react on the right side. In eq. (1), symbols n_0, n_1,… n_r and m_1,… m_s are assigned for the stoichiometric coefficients of the reacting molecules from left and right sides. If $n_0 = 0$ then the solvent is not involved in the chemical reaction and if $n_0 \neq 0$ then the solvent is involved in the reaction. In dilute solutions the following equality $N_i << N_0$ holds true. If we assume that the solution is an ideal solution, then the chemical potential of species *i*, μ_i, can be represented as follows:

$$\mu_i = \mu_i^0 + RT \ln [C_i], \quad (2)$$

where the activity of the species i is defined as $[C_i] = C_i / C_i^0$, C_i is a molar concentration, and C_i^0 is the molar concentration of species i in the standard state. In chemical physics of solutions, the standard state of a solution is considered as a state where there are no interactions between species and their behavior can be assumed as ideal. The standard state is chosen at C_i^0=1M [53].

The equilibrium conditions are obtained using the relation of the Gibbs free energy, ΔG^0, and the constant of chemical reaction, *K*, as [53]:

$$\Delta G^0 = -RT \ln K \quad (3)$$

where R is the gas constant and T is the absolute temperature and the equilibrium constant is expressed using the activities of the species as:

$$K = \frac{[B_1]^{m_1} \ldots [B_s]^{m_s}}{[A_0]^{n_0}[A_1]^{n_1} \ldots [A_r]^{n_r}} \quad (4)$$

In this work, all experiments were performed at the room temperature T=25°C, hence eq.(1) is simplified as $\Delta G^0 = A \log_{10} K$, where $A = -5.71 kJ/mol$ [55-61]. The Gibbs free energies of all possible compounds are collected in **Table 1**.

Consider dissolution of the solid tungsten compounds in an aqueous solution. During dissolution in an aqueous solution, tungsten can form a variety of tungstate ions [53, 62, 63], such as $HW_6O_{21}^{5-}$, $H_2W_{12}O_{42}^{10-}$, $W_6O_{21}^{6-}$, $W_7O_{24}^{6-}$, $W_{12}O_{41}^{10-}$, $H_2W_{12}O_{40}^{6-}$, $W_{12}O_{39}^{6-}$, $W_{10}O_{32}^{4-}$. Due to a limited availability of the Gibbs free energy data and the fact that the $HW_6O_{21}^{5-}$ ion has the lowest Gibbs free energy among the known polytungstate ions, we have restricted ourselves to the analysis involving only this ion. Hence only reactions depending on its presence were chosen for the construction of the diagrams. Possible solid compounds and their aqueous products are listed in **Table 1**. Using the equilibrium conditions for the reactions of tungsten with water, the stability of the compounds can be studied.

Table 1. List of considered compounds and their standard partial molar Gibbs energies. ((s) - solid, (l) - liquid, (aq) - aqueous).

Name	Species (state)	$\Delta \overline{G}_i^0, (kJ/mol)$	References
Tungsten (VI) trioxide	$WO_3(s)$	-763.9	[53, 54]
Tungsten (VI) trioxide monohydrate	$WO_3 \cdot H_2O(s)$	-1020.9	[64]
Tungsten (VI) trioxide dihydrate	$WO_3 \cdot 2H_2O(s)$	-1220.0	[53]
Tungstate (VI) ion	$WO_4^{2-}(aq)$	-916.7	[53]
Polytungstate ion	$HW_6O_{21}^{5-}(aq)$	-5175.6	[53]
Water	$H_2O(l)$	-237.2	[53]
Hydrogen ion	$H^+(aq)$	0.0	[53]

Hydroxide	$OH^-(aq)$	-157.3	[53]

It can be noticed that the equilibrium boundaries separating different aqueous solutions are represented in the form:

$$\alpha\, pH = \beta \log[WO_4^{2-}] + \delta \log[HW_6O_{21}^{5-}] + \gamma \quad (5)$$

where constants $\alpha, \beta, \delta, \gamma$ are given in Table 2 for the particular chemical reactions.

Table 2. The list of $\alpha, \beta, \delta, \gamma$ coefficients.

Compounds pairs	Chemical reactions	α	β	δ	γ
$WO_3(s) / WO_4^{2-}(aq)$	$WO_3 + H_2O = WO_4^{2-} + 2H^+$	2	1	0	14.8
$WO_3(s) / HW_6O_{21}^{5-}(aq)$	$6WO_3 + 3H_2O = HW_6O_{21}^{5-} + 5H^+$	5	1	0	20.9
$HW_6O_{21}^{5-}(aq) / WO_4^{2-}(aq)$	$HW_6O_{21}^{5-} + 3H_2O = 6WO_4^{2-} + 7H^+$	7	6	-1	67.8
$WO_3 \cdot H_2O(s) / WO_4^{2-}(aq)$	$WO_3 \cdot H_2O = WO_4^{2-} + 2H^+$	2	1	0	18.3
$WO_3 \cdot H_2O(s) / HW_6O_{21}^{5-}(aq)$	$6(WO_3 \cdot H_2O) = HW_6O_{21}^{5-} + 3H_2O + 5H^+$	5	1	0	41.7
$WO_3 \cdot 2H_2O(s) / WO_4^{2-}(aq)$	$WO_3 \cdot 2H_2O = WO_4^{2-} + 2H^+ + H_2O$	2	1	0	11.6
$WO_3 \cdot 2H_2O(s) / HW_6O_{21}^{5-}(aq)$	$6(WO_3 \cdot 2H_2O) = HW_6O_{21}^{5-} + 9H_2O + 5H^+$	5	1	0	1.7

Now, equilibrium conditions are plotted in Figure 2 (a, b, c) where $\log C = \log[WO_4^{2-}]$ if tungstate ions WO_4^{2-} are involved in the reaction, or $\log C = \log[HW_6O_{21}^{5-}]$ if the polytungstates $HW_6O_{21}^{5-}$ are involved in the reaction. The regions marked with WO_3, $WO_3 \cdot H_2O$ or $WO_3 \cdot 2H_2O$ specify the concentration-versus-pH conditions when these compounds can be stable with respect to water, meaning that these compounds will stay solid and would not dissolve in water. The regions marked with the polytungstates $HW_6O_{21}^{5-}$ specify the concentration-versus-pH conditions when the solid compounds WO_3, $WO_3 \cdot H_2O$ or $WO_3 \cdot 2H_2O$ will react with water producing the polyions and will eventually dissolve in water producing polytungstates $HW_6O_{21}^{5-}$. And the region marked with the tungstate ions WO_4^{2-} specify the concentration-versus-pH

conditions when the polyions $HW_6O_{21}^{5-}$ will react with water producing the tungstate ions. The straight lines represent the boundaries along which both species from each side of the line can coexist in equilibrium. The OH^- and H^+ lines represent equilibrium conditions at which hydroxyl ion or hydrogen ion will be stable with respect to water.

As an illustration of the application of these diagrams, we use Figure 2 (a) and follow the horizontal dashed arrows from the right to the left. Assume that a solid WO_3 compound is added to an aqueous solution which is maintained at pH14. As follows from this diagram, the WO_3 compound will be dissolved in this solution producing the tungstate ions WO_4^{2-} which are the only stable species at pH14. If some acid is added to this solution and pH is lowered, say to pH7.6, the tungstate ion will react with the hydrogen ion producing polytungstate ion $HW_6O_{21}^{5-}$ and both tungsten ions will be in the equilibrium with each other at this pH point. However, if pH is lowered even more, say to pH6, then the tungstate ions will react to produce polytungstate ions and only polytungstate ions will be present in the system when the system reaches equilibrium. Adding more acid to this solution and lowering the solution pH to pH2, one can force the polytungstate ions to react with the hydrogen ions to produce the tungsten trioxide. The latter will precipitate out as a solid particle. Below this pH, all the polytungstate ions will react to form solid tungsten trioxide.

It is instructive to interpret the effect of ion concentration on the thermodynamic state of the solution following the vertical arrows. If a small amount of the solid tungsten trioxide is added to the beaker with the pure water (pH7), the chemical reaction will proceed with the formation of the tungstate ions and the hydrogen ions. Increasing the amount of solid tungsten trioxide, one would produce more tungstate ions until the concentration of the tungstate ion will reach the

critical concentration $-\log C = -\log[WO_4^{2-}] = 3.8$ or $[WO_4^{2-}] = 10^{-3.8} M$ beyond which the tungstate ions will start reacting with the hydrogen ion producing the polytungstate ions. Above this critical concentration, the tungsten trioxide will continue react with water, forming polytungstate ions instead.

From these diagrams, one infers that the composition of the solution is influenced by the concentration of the ions produced in the electrochemical reaction. Figure 2(d) shows a three dimensional diagram where the planar boundary represents the equilibrium between the polytungstate ions and tungstate ions. Bellow this boundary, the tungstate ion will convert into the polytungstate ion and vice versa to reach the equilibrium.

Analyzing these diagrams, we conclude that the ionic products of tungsten electropolishing will precipitate in the form of the tungsten trioxide monohydrate as the pH level is lowered below ~ pH8 with concentration of tungstate ions around $-\log[WO_4^{2-}] \approx 2.4$. Decreasing pH below pH1, one expects to observe the tungsten trioxide dihydrate as a solid precipitate.

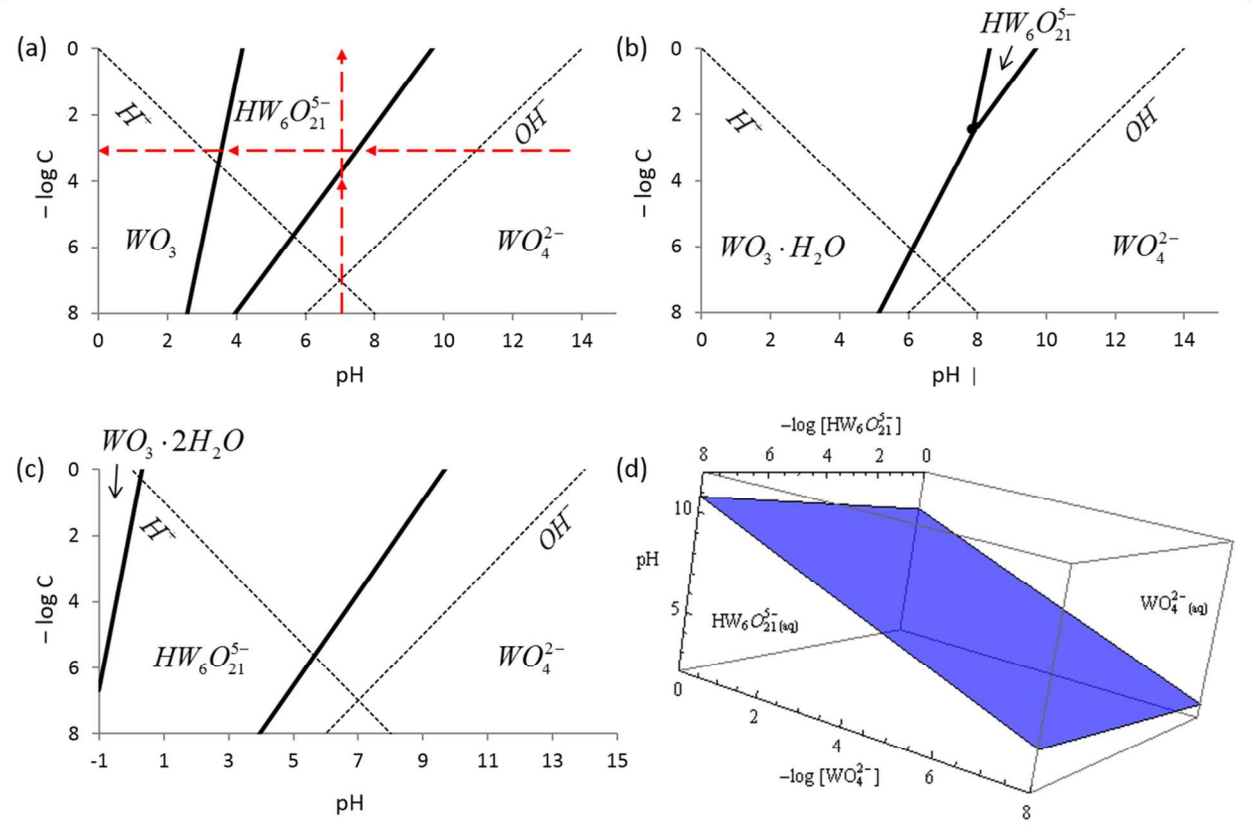

Figure 2. Dependence of –LogC on pH, considering thermodynamic stability of (a) WO_3, (b) $WO_3 \cdot H_2O$ and (c) $WO_3 \cdot 2H_2O$ compounds. (d) Three dimensional graph showing the dependence of $-\log[WO_4^{2-}]$ and $-\log[HW_6O_{21}^{5-}]$ on pH. The concentration C represents the concentration of the ions in the system as explained in the text.

These diagrams suggest that electropolishing should proceed with a change of the electrolyte composition, and, most important, with a possibility of phase separation. In electropolishing of tungsten wires, the wire is submersed in the electrolyte. The CLE regime of electropolishing significantly relies on the complex physico-chemical phenomena occurring under meniscus formed by the electrolyte/air interface around the wire [14]. Since the surface tension is very sensitive to the electrolyte composition [37, 65], it is therefore instructive to develop a theoretical basis for interpretation of the experimental data on the surface tension changes.

Gibbs adsorption isotherm

At constant temperature and pressure, the Gibbs adsorption equation is given as[65]:

$$d\sigma = -\sum_i \Gamma_i d\mu_i, \qquad (6)$$

where Γ_i is the surface excess of the compound i concentrated at the air/liquid interface and measured with respect to the concentration of some compound at a reference surface, μ_i is its chemical potential and σ is the surface tension of the electrolyte. In order to go further and interpret the Gibbs adsorption equation for our case, we first need to specify all possible ions present in the system.

Discussing adsorption phenomena, we cannot ignore a possibility for potassium hydroxide to alter the thermodynamic pathway of chemical reactions. As mentioned, the surface properties of electrolytes are very sensitive to any contaminants. Therefore, while potassium containing compounds are known to quickly dissociate in aqueous solutions [53, 58, 60], their effect on surface properties of solutions is important to investigate.

Effect of potassium hydroxide

In electropolishing of tungsten in potassium hydroxide solution, tungsten consumes hydroxyl groups OH^- producing tungstate ions WO_4^{2-}[24]:

$$W + 2OH^- + 2H_2O = WO_4^{2-} + 3H_2 \qquad (7)$$

Potassium hydroxide dissociates onto potassium ions and hydroxide groups, hence positively charged potassium is able to associate with negatively charged tungstate ions to form a highly water soluble compound K_2WO_4 [66, 67]:

$$2K^+ + WO_4^{2-} = K_2WO_4 \qquad (8)$$

The total concentration C of dissolved species is:

$$C = C_1 + C_2, \tag{9}$$

where C_i is concentrations of the i-th compound, i = 1,2, $C_1 = C_{KOH}$, $C_2 = C_{K_2WO_4}$ measured in mol/L. Following the stoichiometry of the reactions, the total concentration of ions is expressed as follows:

$$\hat{C} = C_{K^+} + C_{OH^-} + C_{WO_4^{2-}} = n_1 C_{KOH} + n_2 C_{K_2WO_4}, \tag{10}$$

where coefficient n_1 is equal to the total number of K^+ and OH^- -ions in the KOH compound and n_2 is equal to the total number of K^+ and WO_4^{2-} ions in the K_2WO_4 compound. If $n_{1K^+}, n_{1OH^-}, n_{2K^+}, n_{2WO_4^{2-}}$ represent the number of ions involved in the process of dissociation of the KOH and K_2WO_4 compounds, we have $n_1 = n_{1K^+} + n_{1OH^-} = 1 + 1 = 2$, $n_2 = n_{2K^+} + n_{2WO_4^{2-}} = 2 + 1 = 3$. Taking into account all reactions occurring in this electrolyte solution, one writes the electro neutrality condition for the solution as: $H^+ + 2OH^- + 3K^+ + WO_4^{2-} = 0$. Now, equation (10) can be rewritten in the following form: $\hat{C} = n_1 C_{KOH} + n_2 C_{K_2WO_4} = 2C_{KOH} + 3C_{K_2WO_4}$. This form prompts one to operate with the concentration of neutral KOH and K_2WO_4 compounds rather than ions.

Motomura used this idea in his studies of complex mixtures [68, 69]. In Motomura's model, the concentration of one ionic component of the mixture is assumed non-changing during adsorption. This assumption is not applicable to the electropolishing case, because, as shown in the previous section, tungsten ions undergo a complex chain of chemical reactions forming different compounds. Therefore, the concentration of the tungsten containing component may not stay unchanged at the air/electrolyte interface. Below, the Motomura model was augmented

to take into account this effect of change of the concentration of potassium and tungstate containing compounds at the air/electrolyte interface.

Following Motomura, we introduce the mole fractions of ions associated with potassium hydroxide ($\hat{X}_1$) and potassium tungstate ($\hat{X}_2$) measured with respect to the total concentration of these ions in these two compounds. Using the defined stoichiometry coefficients, one obtains

$$\hat{X}_1 = \frac{n_1 C_{KOH}}{\hat{C}} = \frac{2C_{KOH}}{2C_{KOH} + 3C_{K_2WO_4}} \tag{11}$$

and

$$\hat{X}_2 = \frac{n_2 C_{K_2WO_4}}{\hat{C}} = \frac{3C_{K_2WO_4}}{2C_{KOH} + 3C_{K_2WO_4}} \tag{12}$$

The introduced mole fractions of ions satisfy the mass balance condition $\hat{X}_1 + \hat{X}_2 = 1$.

Using these definitions and assuming that the solution is ideal, one can write the differentials of the chemical potentials of the ions as:

$$d\mu_{OH^-} = RTd\ln\left[\frac{\hat{C}\hat{X}_1}{n_2}\right] = \frac{RT}{\hat{C}}d\hat{C} + \frac{RT}{\hat{X}_1}d\hat{X}_1. \tag{13}$$

From the mass balance condition $\hat{X}_1 + \hat{X}_2 = 1$ one can find the relation $\hat{X}_1 = 1 - \hat{X}_2$ and hence rewrite eq.(13) as:

$$d\mu_{OH^-} = \frac{RT}{\hat{C}}d\hat{C} - \frac{RT}{\hat{X}_1}d\hat{X}_2. \tag{14}$$

Following the same logic and using eq.(2), the chemical potential of the WO_4^{2-} ions is written as:

$$d\mu_{WO_4^{2-}} = \frac{RT}{\hat{C}}d\hat{C} + \frac{RT}{\hat{X}_2}d\hat{X}_2 \tag{15}$$

The chemical potential of the K^+ ions is then written as:

$$d\mu_{K^+} = \frac{RT}{\hat{C}} d\hat{C} - RT \frac{\frac{n_{1K^+}}{n_1} - \frac{n_{2K^+}}{n_2}}{\frac{n_{1K^+}}{n_1}\hat{X}_1 + \frac{n_{2K^+}}{n_2}\hat{X}_2} d\hat{X}_2 \quad (16)$$

With these chemical potentials, we can derive the Gibbs adsorption isotherm of aqueous solutions of tungsten and potassium mixtures.

Gibbs adsorption isotherm of complex mixtures mixture

Assuming constant pH (this assumption will be verified later in experiments), the Gibbs adsorption equation $H_2O + H^+ + 2OH^- + 3K^+ + WO_4^{2-} = 0$ is expressed as follows:

$$d\sigma = -\Gamma^H_{H_2O} d\mu_{H_2O} - \Gamma^H_{OH^-} d\mu_{OH^-} - \Gamma^H_{WO_4^{2-}} d\mu_{WO_4^{2-}} - \Gamma^H_{K^+} d\mu_{K^+}, \quad (17)$$

where superscript H represents an adsorbed quantity at the air-liquid interface, and symbols $\Gamma^H_{OH^-}, \Gamma^H_{WO_4^{2-}}, \Gamma^H_{K^+}$ represent the number of moles of the adsorbed ions OH^-, WO_4^{2-}, K^+ per unit area at the air-liquid interface.

Due to convention, adsorption of water molecules $\Gamma^H_{H_2O}$ at the air/electrolyte interface is set zero[65, 70], thus eq. (17) is rewritten as:

$$d\sigma = -\Gamma^H_{OH^-} d\mu_{OH^-} - \Gamma^H_{WO_4^{2-}} d\mu_{WO_4^{2-}} - \Gamma^H_{K^+} d\mu_{K^+} \quad (18)$$

The total Gibbs adsorption of all ions at the air-liquid interface is represented as:

$$\hat{\Gamma}^H = \Gamma^H_{OH^-} + \Gamma^H_{WO_4^{2-}} + \Gamma^H_{K^+}, \quad (19)$$

where, $\Gamma^H_{K^+}$ is defined as:

$$\Gamma^H_{K^+} = n_{1K^+}\Gamma^H_1 + n_{2K^+}\Gamma^H_2, \quad (20)$$

where, $\Gamma^H_{OH^-}$ and $\Gamma^H_{WO_4^{2-}}$ are defined as:

$$\Gamma^H_{OH^-} = n_{1OH^-}\Gamma^H_1, \tag{21}$$

and

$$\Gamma^H_{WO_4^{2-}} = n_{2WO_4^{2-}}\Gamma^H_2 \tag{22}$$

The total adsorption of compounds 1 and 2, Γ^H , is written as:

$$\Gamma^H = \Gamma^H_1 + \Gamma^H_2 \tag{23}$$

The mole fraction of the K_2WO_4 compound at the air-liquid interface is then:

$$X^H_2 = \frac{\Gamma^H_2}{\Gamma^H} \tag{24}$$

Using the stoichiometry coefficients, the mole fraction of ions at the air-liquid interface is found as:

$$\hat{X}^H_2 = \frac{\Gamma^H_{WO_4^{2-}} + n_{2c}\Gamma^H_2}{\hat{\Gamma}^H}, \tag{25}$$

Substituting the differentials of the chemical potentials $d\mu_{OH^-}, d\mu_{WO_4^{2-}}, d\mu_{K^+}$ (eq.(14), (15), (16)) into the Gibbs adsorption equation (18), one obtains:

$$d\sigma = -\Gamma^H_{OH^-}\left[\frac{RT}{\hat{C}}d\hat{C} - \frac{RT}{\hat{X}_1}d\hat{X}_2\right] - \Gamma^H_{WO_4^{2-}}\left[\frac{RT}{\hat{C}}d\hat{C} + \frac{RT}{\hat{X}_2}d\hat{X}_2\right] - \Gamma^H_{K^+}\left[\frac{RT}{\hat{C}}d\hat{C} - RT\frac{\frac{n_{1K^+}}{n_1} - \frac{n_{2K^+}}{n_2}}{\frac{n_{1K^+}}{n_1}\hat{X}_1 + \frac{n_{2K^+}}{n_2}\hat{X}_2}d\hat{X}_2\right]. \tag{26}$$

Collecting the same differentials and using eq.(19) and eq.(25), the Gibbs adsorption equation for the complex mixture containing potassium and tungstate ions is written as:

$$d\sigma = -\frac{\hat{\Gamma}^H RT}{\hat{C}}d\hat{C} + \hat{\Gamma}^H RT\frac{\hat{X}_2 - \hat{X}^H_2}{\hat{X}_1\hat{X}_2}\left[1 - \frac{n_{1K^+}n_{2K^+}}{n_{1K^+}n_2\hat{X}_1 + n_{2K^+}n_1\hat{X}_2}\right]d\hat{X}_2, \tag{27}$$

The Gibbs adsorption equation in this form is convenient to use for a practically important case when the concentration of potassium hydroxide does not change significantly. In particularly, at the beginning of tungsten electropolishing, the concentration of potassium hydroxide can be considered constant because the concentration of potassium tungstate goes to zero, $\hat{X}_2 \to 0$. We discuss this important case below.

Evaluation of the total amount of adsorbate at the air/electrolyte interface at low concentration of potassium tungstate

Assuming constant concentration of potassium hydroxide, C_{KOH}, the differential of eq.(12) is written as

$$d\left(\hat{X}_2\hat{C}\right) = n_2 dC_{K_2WO_4} \tag{28}$$

Accordingly, the differential of total concentration of compounds is rewritten in the form:

$$d\hat{C} = n_2 dC_{K_2WO_4} \tag{29}$$

Therefore, eq. (28) is expanded as $\hat{X}_2 n_2 dC_2 + \hat{C}d\hat{X}_2 = n_2 dC_2$, leading to the following relation:

$$n_2 dC_{K_2WO_4} = d\hat{C} = -\frac{\hat{C}}{\left(\hat{X}_2 - 1\right)} d\hat{X}_2, \Rightarrow, \frac{d\hat{C}}{\hat{C}} = -\frac{d\hat{X}_2}{\left(\hat{X}_2 - 1\right)} \tag{30}$$

Substituting eq.(30) into the first term on the right hand side of eq.(27), one:

$$\frac{d\sigma}{d\hat{X}_2} = \frac{\hat{\Gamma}^H RT}{(\hat{X}_2 - 1)} + \hat{\Gamma}^H RT \frac{\hat{X}_2 - \hat{X}_2^H}{\hat{X}_1 \hat{X}_2}\left[1 - \frac{n_{1K^+} n_{2K^+}}{n_{1K^+} n_2 \hat{X}_1 + n_{2K^+} n_1 \hat{X}_2}\right] \tag{31}$$

At low concentration of the potassium tungstate, when $\hat{X}_2 \to 0$, eq.(31) is simplified as:

$$\left.\frac{d\sigma}{d\hat{X}_2}\right|_{\hat{X}_2 = 0} = -\hat{\Gamma}^H RT + \frac{\hat{\Gamma}^H RT}{\hat{X}_1}\left[1 - \frac{n_{1K^+} n_{2K^+}}{n_{1K^+} n_2 \hat{X}_1}\right]|_{\hat{X}_1 = 1}, \tag{32}$$

to provide the total amount of adsorbate $\hat{\Gamma}^H$ as:

$$\hat{\Gamma}^H = \frac{d\sigma}{d\hat{X}_2} \frac{1}{RT\left(-1+\frac{1}{\hat{X}_1}-\frac{n_{1K^+}n_{2K^+}}{n_{1K^+}n_2\hat{X}_1^2}\right)}\Big|_{\hat{X}_1=1} = -\frac{d\sigma}{d\hat{X}_2}\frac{n_{1K^+}n_2}{RT\cdot n_{1K^+}n_{2K^+}} \quad (33)$$

Plugging $n_1 = n_{1_{K^+}} + n_{1OH^-} = 1+1 = 2, n_2 = n_{2K^+} + n_{2WO_4^{2-}} = 2+1 = 3$ into this equation, the total Gibbs adsorption $\hat{\Gamma}^H$ at the air/electrolyte interface in this limiting case is calculated as:

$$\hat{\Gamma}^H = -\frac{d\sigma}{d\hat{X}_2}\cdot\frac{3}{2RT} \quad (34)$$

Thus, in order to evaluate the total amount of adsorbate, one needs to find the slope $d\sigma/d\hat{X}_2$ of the surface tension versus potassium tungstate concentration at low concentration of the latter.

RESULTS AND DISCUSSION

The solutions prepared using PLE regime with tungsten plate electropolished in KOH solution was used to conduct the proposed studies on change of solution properties upon dissolution of tungsten. Table 3 shows the following data collected from electropolishing experiment at time t: total charge Q, mass of the electrochemical products WO_4^{2-} released into electrolyte $m_{WO_4^{2-}}$ and calculated using Faraday's law, density ρ of the solution measured using microbalance and micropipette, concentration $C_{WO_4^{2-}}$ of the reaction products WO_4^{2-}, surface tension measured using the drop shape analyzer, the concentration of KOH, C_1, in the electrolyte, the concentration of K_2WO_4, C_2. Parameters $\hat{C}$, $\hat{X}_1$, $\hat{X}_2$ were calculated using equations presented above (10), (11), (12), respectively. The K_2WO_4 concentration was determined using eq.(8), where concentrations of K_2WO_4 and WO_4^{2-} come in the 1:1 ratio.

Table 3. Experimental data and calculated parameters for the tungstate solutions.

t, s	Q, C	$m_{WO_4^{2-}}$, g	ρ, g/cm^3	$C_{WO_4^{2-}}$,mol/L	σ, mN/m	C_1	C_2	$\hat{C}$	$\bar{X}_1$	$\bar{X}_2$
0	0	0.000	1.085	0.00	75.18	2.00	0.00	4.00	1.00	0.00
50	11	0.003	1.091	0.02	74.70	2.00	0.02	4.07	0.98	0.02
100	19	0.006	1.101	0.06	74.28	2.00	0.06	4.19	0.95	0.05
200	37	0.012	1.109	0.10	73.81	2.00	0.10	4.30	0.93	0.07
300	51	0.016	1.127	0.19	73.56	2.00	0.19	4.57	0.88	0.12
600	91	0.029	1.170	0.34	72.98	2.00	0.34	5.03	0.80	0.20
470	150	0.047	1.149	0.28	73.30	2.00	0.28	4.84	0.83	0.17
1000	182	0.057	1.206	0.49	73.20	2.00	0.49	5.47	0.73	0.27
2000	332	0.105	1.228	0.58	73.57	2.00	0.58	5.74	0.70	0.30
6100	356	0.113	1.224	0.65	73.26	2.00	0.65	5.96	0.67	0.33

Figure 3 collects the results of the surface tension and pH measurements of the tungstate solutions prepared by electropolishing of tungsten in the potassium hydroxide electrolyte. The inserts in Figure 3 shows a sequence of images of the solutions prepared by electropolishing of tungsten in the 2M KOH electrolyte for different periods of time. Remarkably, the pH of the potassium hydroxide with tungstate ions solutions remains almost constant when the surface tension visibly decreases. The constancy of pH provides the solid ground for the theory of the Gibbs adsorption isotherm that we derived, eq. (34).

Manifestation of thermodynamic instability of electrolytes during electropolishing

The pH drops from pH14 to pH9 at the 0.65M concentration of the tungstate ions when the surface tension has already stabilized. These observations confirm the presence of precipitates as

suggested by the phase diagrams that we constructed earlier. These diagrams also suggest that the tungstate ions should form the $WO_3 \cdot H_2O$ precipitates when pH drops below pH8, which is in agreement with the observations.

As shown in the Supporting Information, the results from the EDS analysis point to the presence of the tungsten oxides/hydrates in the precipitates. The thermal analysis revealed the presence of the structurally bound or hydrated water. This indicates that the precipitates are most likely consisting of tungsten hydrates that are present in the amorphous form.

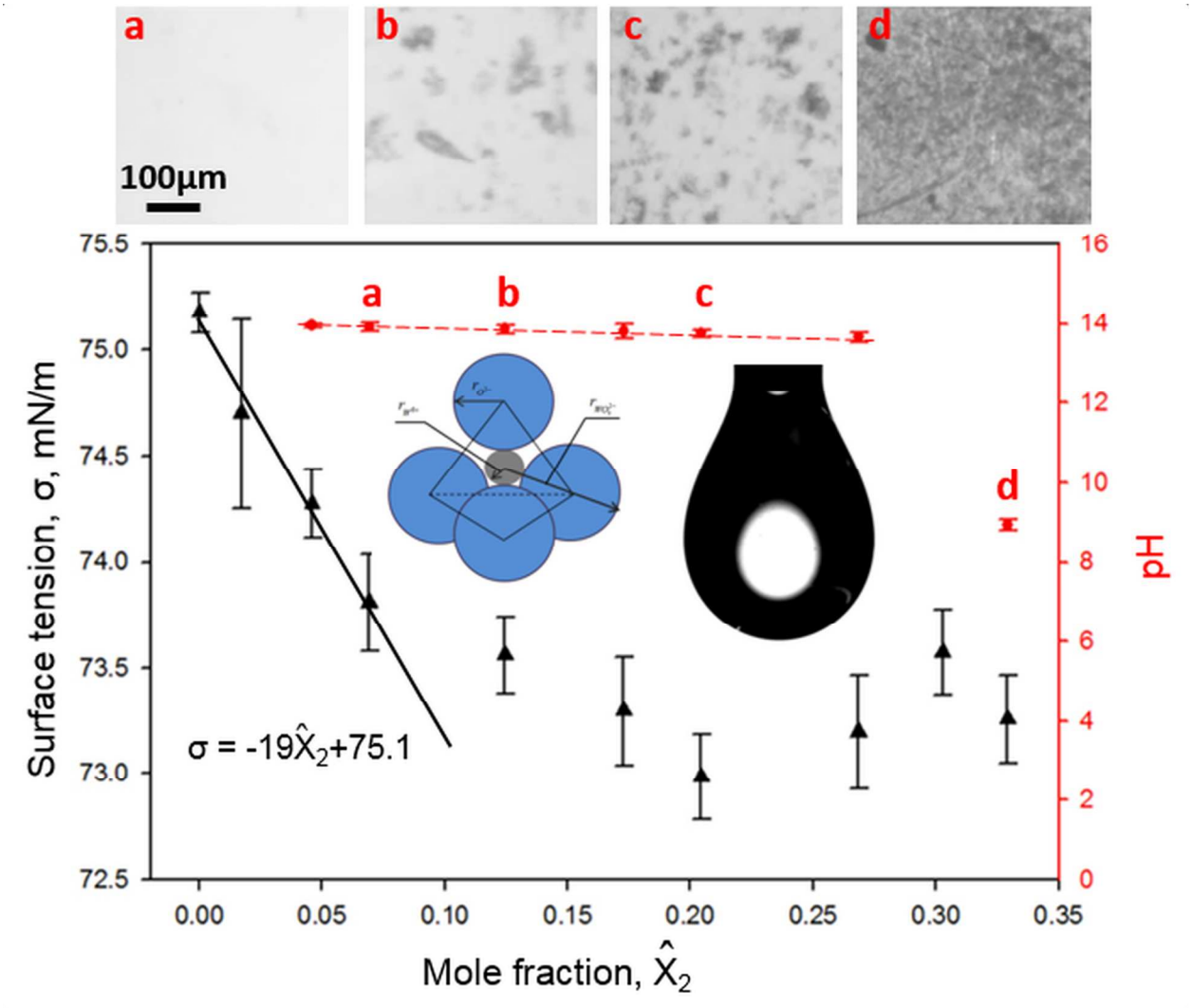

Figure 3. Surface tension (black triangles) and pH (red diamonds) as a function of the K_2WO_4 concentration. The inserts are optical images of the mixtures.

The presence of precipitates significantly changes rheological properties of electrolyte especially near the wire surface. As shown in ref. [14], in the CLE, a thin liquid film with distinguishable properties is formed near the wire surface. We followed the same CLE protocol to X-ray film the process. The tungsten wire was electropolished until the lower part of the wire immersed into the liquid was dropped off and meniscus that was originally created on the wire, slid off the wire exposing the needle to the air. At this moment, the wire was imaged using TXM mosaic mode, where 15 images with 40 x 40 μm^2 field of view were collected consequently and combined together automatically to form an expanded image that is shown in **Figure 4** (a). After that the wire was left undisturbed in the tube for 1 h for stabilization of the electrolyte; then the X-ray nanotomography was performed. The result of the nanotomography is shown in **Figure 4** (b).

In contrast to the recently discovered regime of electropolishing leading to formation of a porous shell[23], the nanotomography of the CLE tip reveals a smooth surface of the tungsten tip without any porous shell, **Figure 4**. Surprisingly, we detected a micrometer thin (diameter d ~ 2μm) bridge connecting suspended part of the wire with the free surface of the liquid spanning about 70 μm distance of the observation spot. The bridge appeared to have some trapped nuclei that remained intact during the nanotomography scan. It should be noted that the bridge was present in the mosaic image that was done immediately after the meniscus had slid down and remained stable until the end of the nanotomography scan.

Prior to the X-ray scanning, the tube with the suspended wire was left in the air. It can be assumed that water from the bridge evaporated during this period of time. According to our analysis of thermodynamic stability of these solutions, evaporation of water, resulting in an increase of the ion concentration, should also lead to the precipitation of tungsten compounds. This explains the presence of particles in the bridge.

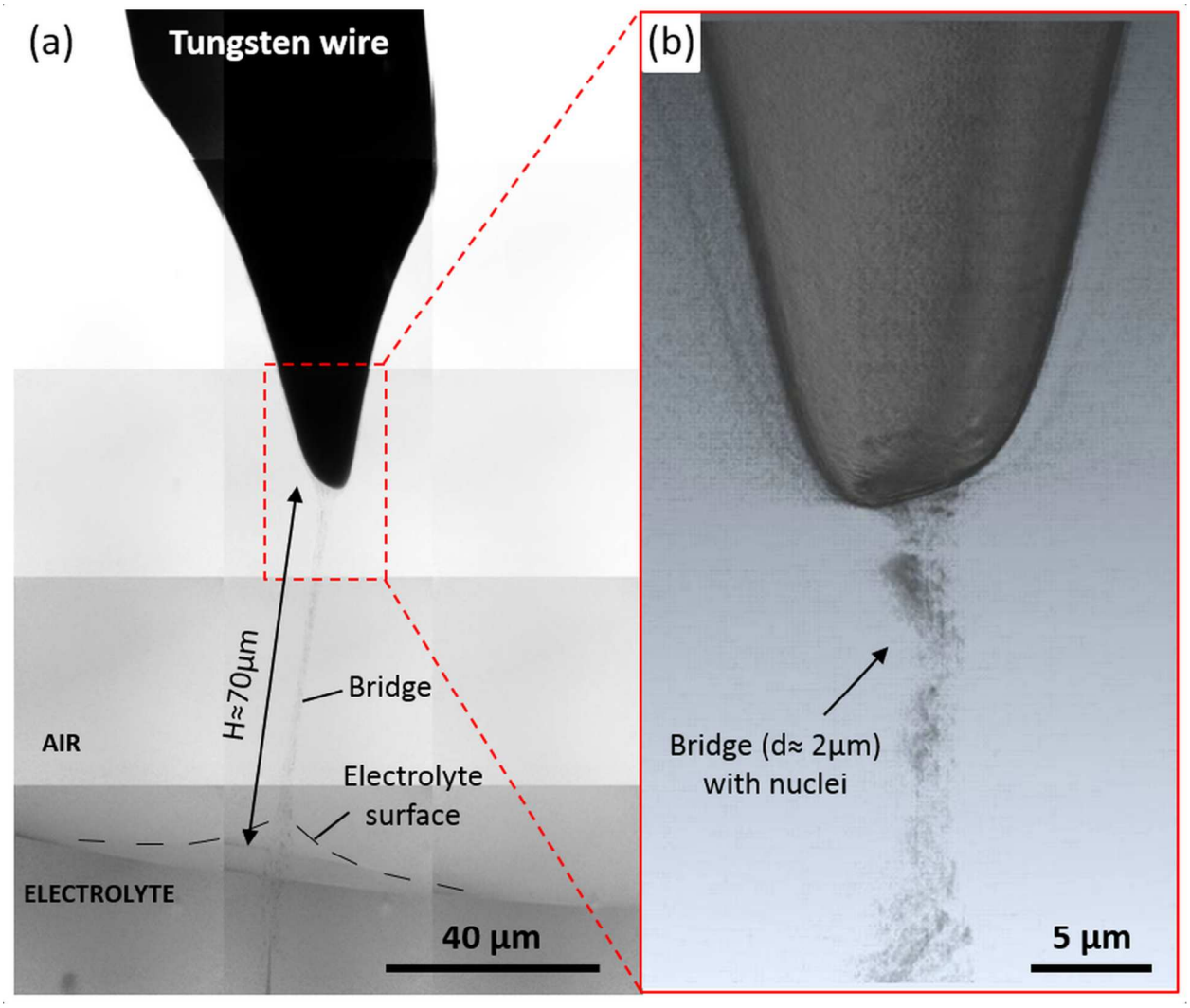

Figure 4. The TXM mosaic image on the left (a) depicts the region where the nanotomography was performed. The image in the red box (b) is a 3D volume rendering view of the reconstructed CLE prepared tip with a bridge connecting the tip with the electrolyte surface.

If we assume that the bridge has the same surface tension as that of the electrolyte, then using **Figure 4** one can estimate the Young's modulus E of the bridge balancing the capillary pressure with the radial stress $\sigma_{rr} \approx E$. Therefore, the order of magnitude estimate gives:

$$E = \frac{2\sigma}{d} = \frac{2 \cdot 73 mN/m}{2\mu m} = 73 kN/m^2 \tag{35}$$

Such a value of the Young's modulus corresponds to a gel-like structure. For example alginate hydrogels have the same order of magnitude moduli [71, 72]. This estimate suggests that the bridge is not completely dried but is formed from a gel-like structure of polytungstates reinforced with the nuclei of different tungsten compounds and bound water. If the bridge were made of tungsten oxides or hydrates, the Young's modulus would be much greater.

Analysis of surface composition of electrolytes

Now, using eq. (34) and knowing the slope $d\sigma / d\hat{X}_2 = -0.019$ from Figure 3, the Gibbs adsorption can be estimated as $\hat{\Gamma}^H = 1.2 \cdot 10^{-5} mol/m^2$. Thus, the Gibbs adsorption appears positive in contrast to the initial Gibbs adsorption of the KOH solution which is negative. This means that the tungstate ions were adsorbed at the surface decreasing the surface tension of the entire mixture.

Knowing the value of the total Gibbs adsorption at the initial point when $\hat{X}_2 = 0$, area A at the surface occupied by a single ion can be found using the following equation:

$$A = \frac{1}{N_A \cdot \hat{\Gamma}^H} = 0.14 nm^2, \tag{36}$$

where N_A is the Avogadro's number $N_A = 6.02 \cdot 10^{23}$ mol^{-1}.

Average area of the tungstate ion. The tungstate ion is a polyatomic ion that consists of four oxygen atoms that surround one tungsten atom that is positioned in the center of the ion. When ions are formed, the atoms arrange themselves in the way to lower the internal energy of the system[73]. To achieve that, they form the three dimensional units, arranging atoms using covalent bonding with the shortest length. In the case of tungstate ion, we have four atoms of oxygen and the optimal configuration for this ion is a tetrahedral arrangement of atoms that is shown in the insert in Figure 3. The ionic radii of oxygen and tungsten ions can be found in literature: $r_{O^{2-}} = 0.13nm$ [55], $r_{W^{6+}} = 0.042nm$ [73]. The tungstate ion radii then can be approximated as $r_{WO_4^{2-}} = r_{W^{6+}} + 2r_{O^{2-}} = 0.302nm$.

Assume that one tungstate ion positioned at the air-liquid interface with one oxygen atom pointing out towards the air with the rest of the oxygen atoms pointing inwards and the next tungstate ion sitting at the air-liquid interface with three oxygen atoms pointing towards the air and one oxygen atom pointing into the liquid. In this case, the area occupied by two tungstate ions at the interface can be approximated by the cross section of the four oxygen atoms. The cross section of a single oxygen atom found as $A_{O^{2-}} = \pi r_{O^{2-}}^2 = 0.053nm^2$. Now, two tungsten ions situated at the air-liquid interface would occupy the area $A_{2ions} = 4A_{O^{2-}} = 0.212nm^2$. Thus, the average area occupied by a single tungstate ion is $A_{ion} = 0.106nm^2$. Comparing the average area occupied by a single ion at the air-liquid interface estimated from the Gibbs adsorption isotherm eq. 36 and the average area of the tungstate ion situated at the air-liquid interface, we conclude that the ions are closely packed at the free liquid surface.

CONCLUSIONS

Theoretical analysis of thermodynamic equilibrium of three solid compounds of tungsten in aqueous solutions of potassium hydroxide allowed one to obtain the solubility conditions of these compounds. In a basic solution with the pH level around pH14, no precipitates can form. When pH is lowered to pH8, the tungsten trioxide monohydrate $WO_3 \cdot H_2O$ might precipitate in the solution. If pH is lowered further to pH4, the tungsten trioxide WO_3 might precipitate. And if pH drops below pH1, the tungsten trioxide dehydrate $WO_3 \cdot 2H_2O$ has a chance to precipitate. We went further to analyze the Gibbs adsorption isotherms of these electrolytes modifying the Motomura theory of surface adsorption of ions at the liquid surfaces.

In order to check the predictions of the derived phase diagrams and analyze the surface tensions of electrolytes, we conducted a series of different experiments. The complex multicompound ionic mixtures consisting of dissociated KOH and tungstate ions in water were studied. With increase of the concentration of tungstate ions, the initially clear solutions changed to turbid indicating the onset of phase separation. Along with this visible change of the solution composition, the surface tension changed as well; it decreased and then stabilized at a lower value relative to the initial level corresponding to the aqueous solution of KOH. Using the Gibbs adsorption isotherm, we provided an estimate of the packing density of ions at the air/liquid interface.

The Gibbs adsorption of potassium ions at the water/air interface was found to be negative. This implies that the ions are repelled from the surface increasing the surface tension as the KOH concentration increases. Analyzing surface tension of the mixture after electropolishing of tungsten in potassium hydroxide solutions, the Gibbs adsorption of tungstate ions was found positive. Thus, the tungstate ions produced during electropolishing are attracted to the air-liquid interface changing the surface adsorption and the surface tension of the mixture.

Characterization of the precipitates revealed that the precipitates are possibly consisting of amorphous tungsten hydrates. The X-ray diffraction revealed the amorphous nature of the precipitates and the energy dispersive X-ray spectroscopy showed the presence of the oxygen in the sample. Finally, thermal analysis revealed the presence of the structurally bounded water implying that the precipitates consist of some type of tungsten hydrate.

Also, using transmission X-ray nanotomography we discovered that the boundary layer of the electrolyte which has distinguishable physical properties, can flow down the electropolished tip and, when exposed to air, it forms a long living gel-like bridge. This bridge showed a remarkable stability: it stayed unbroken for about two hours after the electrochemical reaction has been stopped. Thus, the oversaturate solution of the products of electrochemical reaction of tungsten and aqueous solution of potassium hydroxides is able to form a gel-like long living structure.

ASSOCIATED CONTENT

Supporting Information

Composition and thermal analysis of the precipitates are presented with EDS, XRD, DSC and TGA data. This material is available free of charge via the Internet at http://pubs.acs.org.

AUTHOR INFORMATION

Corresponding Author

*E-mail: KKORNEV@clemson.edu

ACNOWLEDGMENTS

We would like to acknowledge the help of Dr. Colin McMillen with the XRD experiments, George Wetzel for his assistance with the SEM and EDS techniques, and Kim Ivey for her help with the thermal analysis techniques. We thank Ella Marushchenko for drawing of Figure 1. Use of the National Synchrotron Light Source, Brookhaven National Laboratory, was supported by the U.S. Department of Energy, Office of Science, Office of Basic Energy Sciences, under Contract No. DE-AC02-98CH10886.

REFERENCES

1. D. Landolt, *Electrochimica Acta*, 1987, 32, 1-11.
2. D. Landolt, P. F. Chauvy and O. Zinger, *Electrochimica Acta*, 2003, 48, 3185-3201.
3. D. Landolt, P. F. Chauvy and O. Zinger, *Electrochimica Acta*, 2004, 49, 2057-2057.
4. Y. Peng, T. Cullis, G. Mobus, X. J. Xu and B. Inkson, *Nanotechnology*, 2009, 20.
5. M. Cavallini and F. Biscarini, *Rev Sci Instrum*, 2000, 71, 4457-4460.
6. C. Williams and D. Roy, *J Vac Sci Technol B*, 2008, 26, 1761-1764.
7. C. Zhang, B. Gao, L. G. Chen, Q. S. Meng, H. Yang, R. Zhang, X. Tao, H. Y. Gao, Y. Liao and Z. C. Dong, *Rev Sci Instrum*, 2011, 82.
8. M. O. Watanabe and T. Kinno, *Appl Surf Sci*, 1994, 76, 353-358.
9. L. Libioulle, Y. Houbion and J. M. Gilles, *Rev Sci Instrum*, 1995, 66, 97-100.
10. W. T. Chang, I. S. Hwang, M. T. Chang, C. Y. Lin, W. H. Hsu and J. L. Hou, *Rev Sci Instrum*, 2012, 83.
11. M. K. Yapici and J. Zou, *Microsyst Technol*, 2008, 14, 881-891.
12. K. Yum, N. Wang and M. F. Yu, *Nanoscale*, 2010, 2, 363-372.
13. M. Kulawik, M. Nowicki, G. Thielsch, L. Cramer, H. P. Rust, H. J. Freund, T. P. Pearl and P. S. Weiss, *Rev Sci Instrum*, 2003, 74, 1027-1030.
14. M. Kulakov, I. Luzinov and K. G. Kornev, *Langmuir*, 2009, 25, 4462-4468.
15. J. E. McKendry, C. S. Allen, K. Critchley, M. L. Gorzny, A. S. Walton and S. D. Evans, *Nanotechnology*, 2008, 19.
16. T. Hryniewicz, R. Rokicki and K. Rokosz, *Surface & Coatings Technology*, 2008, 202, 1668-1673.
17. Z.-W. Fan and L.-W. Hourng, *International Journal of Machine Tools & Manufacture*, 2009, 49, 659-666.
18. R. Rokicki and T. Hryniewicz, *Trans. Inst. Metal Finish.*, 2012, 90, 188-196.
19. I. Ekvall, E. Wahlstrom, D. Claesson, H. Olin and E. Olsson, *Meas Sci Technol*, 1999, 10, 11-18.
20. A. Nakata, T. Nomoto, T. Toyota and M. Fujinami, *Anal. Sci.*, 2013, 29, 865-869.
21. J. C. Grunlan, X. Y. Xia, D. Rowenhorst and W. W. Gerberich, *Rev Sci Instrum*, 2001, 72, 2804-2810.

22. T. T. Hironori Tohmyoh, Masato Fujimori and Masumi Saka *J. Micro Nano-Manuf.*, 2013, 1.
23. M. Nave, B. Rubin, V. Maximov, S. Creager and K. G. Kornev, *Nanotechnology*, 2013, 24, 355702.
24. G. S. Kelsey, *Journal of the Electrochemical Society*, 1977, 124, 814-819.
25. K. Ali, H. Anwar ul, S. Bilal and S. Siddiqi, *Colloid Surf. A-Physicochem. Eng. Asp.*, 2006, 272, 105-110.
26. P. M. Wang, A. Anderko and R. D. Young, *Ind. Eng. Chem. Res.*, 2011, 50, 4086-4098.
27. V. S. Markin and A. G. Volkov, *J. Phys. Chem. B*, 2002, 106, 11810-11817.
28. Y. Marcus, *J. Chem. Eng. Data*, 2010, 55, 3641-3644.
29. B. C.-Y. L. Zhibao Li, *Chemical Engineering Science*, 2001, 56, 2879-2888.
30. R. I. Slavchov and J. K. Novev, *J. Colloid Interface Sci.*, 2012, 387, 234-243.
31. K. J. Mysels, *Langmuir*, 1986, 2, 423-428.
32. A. U. A. Shah, K. Ali and S. Bilal, *Colloid Surf. A-Physicochem. Eng. Asp.*, 2013, 417, 183-190.
33. K. Ali, A. Shah, S. Bilal and H. Azhar ul, *Colloid Surf. A-Physicochem. Eng. Asp.*, 2008, 330, 28-34.
34. K. Ali, A. Shah and S. Bilal, *Colloid Surf. A-Physicochem. Eng. Asp.*, 2009, 337, 194-199.
35. J. Drzymala and J. Lyklema, *J Phys Chem A*, 2012, 116, 6465-6472.
36. A. W. Adamson, ed., *Physical chemistry of surfaces*, A Wiley-Interscience publication, New York, 1990.
37. N. Matubayasi, ed., *Surface tension and related thermodynamic quantities of aqueous electrolyte solutions*, (CRC Press Taylor&Francis Group, 2014.
38. P. K. Weissenborn and R. J. Pugh, *Langmuir*, 1995, 11, 1422-1426.
39. P. B. Petersen, J. C. Johnson, K. P. Knutsen and R. J. Saykally, *Chem. Phys. Lett.*, 2004, 397, 46-50.
40. I. Langmuir, *Science (New York, N.Y.)*, 1938, 88, 430-432.
41. P. B. Petersen and R. J. Saykally, *J. Am. Chem. Soc.*, 2005, 127, 15446-15452.
42. M. Dole, 1938, 60.
43. G. R. Jones, W.A., *J. Am. Chem. Soc.*, 1935, 57, 957-958.
44. G. R. Jones, W.A., *J. Am. Chem. Soc.*, 1937, 59, 187-198.
45. G. R. Jones, W.A., 1941, 63, 288-294.
46. G. R. Jones, W.A., *J. Am. Chem. Soc.*, 1941, 63, 3262-3263.
47. G. R. Jones, W.A., *J. Am. Chem. Soc.*, 1942, 64, 2744-2745.
48. K. A. Karraker and C. J. Radke, *Adv. Colloid Interface Sci.*, 2002, 96, 231-264.
49. P. B. Costa Akerlof, *J. Am. Chem. Soc.*, 1941, 63, 1085-1088.
50. P. Jungwirth and D. J. Tobias, *Chem. Rev.*, 2006, 106, 1259-1281.
51. J. Wang, Y. C. K. Chen, Q. X. Yuan, A. Tkachuk, C. Erdonmez, B. Hornberger and M. Feser, *Applied Physics Letters*, 2012, 100.
52. F. Natterer, *The Mathematics of Computerized Tomography*, Wiley, New York.
53. G. K. Schweitzer and L. L. Pesterfield, *The aqueous chemistry of the elements*, Oxford University Press, Oxford ; New York, 2010.
54. P. Pradyot, *Handbook of inorganic chemicals*, McGraw-Hill Professional, 2002.
55. J. V. Walther, *Essentials of Geochemistry*, Jones and Bartlett Publishers, Sudbury, Massachusetts, 2005.

56. D. K. Nordstrom and J. L. Munoz, *Geochemical Thermodynamics*, Blackwell Scientific Publications, Boston, Second Edition edn., 1994.
57. T. R. Blackburn, *Equilibrium A Chemistry of Solutions*, (Holt, Rinehart and Winston, Inc., 1969.
58. G. M. Anderson and D. A. Grerar, *Thermodynamics in Geochemistry*, Oxford University Press, Inc., New York, 1993.
59. J. M. Smith, H. C. Van Ness and M. M. Abbott, *Introduction to Chemical Engineering Thermodynamics*, McGraw-Hill New York, Sixth edn., 2001.
60. D. Langmuir, *Aqueous Environmental Geochemistry*, Prentice-Hall, Inc., 1997.
61. E. Fermi, *Thermodynamics*, Prentice-Hall, Inc., New York, 1937.
62. K.-c. i. Li and C. u.-y. Wang, *Tungsten: its history, geology, ore-dressing, metallurgy, chemistry, analysis, applications, and economics*, Reinhold, New York,, 3d edn., 1955.
63. M. T. Pope, *Heteropoly and isopoly oxometalates*, Springer-Verlag, Berlin ; New York, 1983.
64. K. Osseo-Asare, *Metallurgical Transactions B*, 1982, 13B, 555-564.
65. A. W. Adamson and A. P. Gast, *Physical chemistry of surfaces*, Wiley, New York, 1997.
66. Z. G. Karov, I. Y. Khochuev, I. N. Lepeshkov and L. I. Karaeva, *Russian Journal of Inorganic Chemistry*, 1989, 34, 1681-1684.
67. T. A. D. N.A.Korotchenko, G.A.Bogdanov and L.I.Zakharkina, *Russian Journal of Inorganic Chemistry*, 1975, 20, 1241-1243.
68. K. Ogino and M. Abe, *Mixed Surfactant Systems*, Marcel Dekker, Inc., New York.
69. K. Motomura, N. Ando, H. Matsuki and M. Aratono, *J. Colloid Interface Sci.*, 1990, 139, 188-197.
70. K. Motomura, *J. Colloid Interface Sci.*, 1978, 64, 348-355.
71. E. Papajova, M. Bujdos, D. Chorvat, M. Stach and I. Lacik, *Carbohydr. Polym.*, 2012, 90, 472-482.
72. M. C. Darnell, J. Y. Sun, M. Mehta, C. Johnson, P. R. Arany, Z. G. Suo and D. J. Mooney, *Biomaterials*, 2013, 34, 8042-8048.
73. J. Samuel, C. J. Brinker, L. J. D. Frink and F. van Swol, *Langmuir*, 1998, 14, 2602-2605.